

# Numerical Investigation on Torsional Mode Self-Excited Vibration of Guide Vane in a Reversible Pump-Turbine during Pump Mode's Starting Up

W. Kang <sup>1</sup>, Q. Liang <sup>2</sup>, L. Zhou <sup>1,3†</sup> and Z. Wang <sup>4</sup>

<sup>1</sup> College of Water Resources and Civil Engineering, China Agricultural University, Beijing, 100083, China

<sup>2</sup> Research & Test Center, Dongfang Electric Machinery Co., Ltd., Deyang, Sichuan Province, 618000, China

<sup>3</sup> Beijing Engineering Research Center of Safety and Energy Saving Technology for Water Supply Network System, Beijing, 100083, China

<sup>4</sup> Department of Energy and Power Engineering, Tsinghua University, Beijing, 100084, China

†Corresponding Author Email: [zlj@cau.edu.cn](mailto:zlj@cau.edu.cn)

(Received April 24, 2022; accepted July 10, 2022)

## ABSTRACT

In reversible pump-turbines, guide vane vibrations are considered to have potentially severe consequences of noise and structural damage. Unstable torsional mode self-excited vibrations of guide vanes have been reported at small guide vane openings during transient operations involving pump flow, such as pump starting and closing processes. In this study, coupling simulations were carried out under different operating conditions based on the unsteady computational fluid dynamics (CFD) method with a single-degree-of-freedom (1DOF) oscillator. The results show that the operating conditions, including the initial opening angle and the pressure difference between the runner side and the stay vane side, significantly affect the instability of guide vane torsional mode self-excited vibration. Energy-based analysis indicates that the positive cumulative work done by total hydraulic torque is responsible for unstable torsional mode self-excited vibration. Furthermore, the relatively small phase difference between total hydraulic torque and guide vane angular velocity, and the positive feedback between vibration amplitude and energy accumulation, are considered to be the root causes that eventually induce unstable self-excited vibrations under the operating conditions of small opening angles and high pressure differences.

**Keywords:** Reversible pump-turbine; Guide vane; Torsional mode; Self-excited vibration; Numerical simulation.

## NOMENCLATURE

$C_v$	velocity coefficient, $C_v = v/U_1$	$R_l$	runner inlet radius
$C_p$	static pressure coefficient, $C_p = p_s / (0.5\rho U_1^2)$	$U_1$	circumferential velocity at runner inlet (m/s), $U_1 = 2\pi n R_l / 60$
$C_\tau$	total hydraulic torque coefficient on guide vane, $C_\tau = \tau / (MgR_l)$	$v$	velocity
$g$	gravitational acceleration	$W_g$	for the dimensionless of the work (N·m·degree), $W_g = \pi MgR_l / 180$
$M$	mass of a guide vane	$\delta\psi$	guide vane inlet-outlet pressure difference, $\delta\psi = (p_{r1} - p_{s2}) / (0.5\rho U_1^2)$
$n$	rotating speed of runner	$\rho$	density of the fluid
$p_s$	static pressure	$\tau$	total hydraulic torque on guide vane
$p_{s2}$	static pressure at guide vane outlet		
$p_{r1}$	total pressure at guide vane inlet		

## 1. INTRODUCTION

Hydropower pumped-storage technology plays a significant role in commercial energy storage at present. Pumped-storage power stations are

employed for load-leveling and grid frequency regulation (Rau 1994). As the key component in a pumped-storage power station, a reversible pump-turbine is used for energy accommodation in pump mode and power generation in turbine mode. Guide

vanes are installed between the runner and the stay vanes for flow guidance and discharge regulation (Tanaka and Tsunoda 1980; Oishi and Yokoyama 1980). Because of the complex and varying operation conditions caused by frequent starting and stopping, undesirable flow patterns and hydraulic instabilities often occur inside a pump-turbine (Zuo *et al.* 2015; Zhang *et al.* 2017; Li *et al.* 2017). With more pump-turbines adopting higher heads and larger unit capacities, these hydraulic instabilities are more likely to induce mechanical vibrations and even premature mechanical failures in extreme cases (Li *et al.* 2017).

Guide vane vibrations in prototype pump-turbines have been widely studied (Pulpitel 1982; Nennemann and Parkinson 2010; Roth *et al.* 2010; 2011; Nennemann *et al.* 2012). Rotor-stator interactions, rotating stalls, and von Karman vortex shedding may cause guide vane vibrations with different frequencies within a normal steady-state operating range. In addition, high-amplitude guide vane vibrations with special frequencies have occurred in some high-head prototype reversible pump-turbines during transient processes such as pump starting, pump closing, and turbine-mode over-speed tests (Nennemann and Parkinson 2010; Nennemann *et al.* 2012; Zuo *et al.* 2015). These guide vane vibrations have typically been found to have large amplitudes around the torsional mode natural frequency in water. Furthermore, high-amplitude fluctuations of pressure and guide vane torque have been observed in situations in which the pressure was measured at the radial gap between guide vanes and runner and the guide vane torque was approximated from the servo pressures (Nennemann and Parkinson 2010). Similar phenomena have been observed in recent starting up tests of a high-head prototype reversible pump-turbine. The horizontal vibrations of the guide vanes and the pressure fluctuations in the radial gap area clearly occurred at high amplitudes of approximately the torsional mode natural frequency of the guide vane in water. Considering the frequent transient operations that occur in pumped-storage power stations that are regulated daily and weekly, this high-amplitude guide vane vibration poses a high risk of collision with neighboring guide vane blades and might lead to structural damage to the hardware and even premature mechanical failures in extreme cases.

Analysis of Nennemann and Parkinson (2010) showed that these special guide vane vibration incidents, which occur in different operating modes, are related to two phenomena of pump flow through small openings: an unstable flow regime caused by the attached flow on the guide vane trailing edge and torsional mode self-excited vibration. According to Tao *et al.* (2019), the flow regime is related to the critical flow rate with respect to the guide vane opening. The flow attachment to the guide vane trailing edge normally appeared when the flow rate was smaller than the critical value. For high-head prototype reversible pump-turbines, a high pressure level at the runner outlet is needed before opening the guide vanes to achieve an efficient starting up

process. This leads to a relatively large flow rate through two guide vane blades and poses a higher risk of torsional mode self-excited vibration, especially at small openings.

Some experimental results and a theoretical model for guide vane self-excited vibrations were presented by Pulpitel (1982). However, some simplified setups and assumptions were employed in this study, such as not fully considering the influence of the circumferential settings and geometric shape of the guide vanes. In contrast, numerical simulations of fluid-structure interaction have been used to study many fluid-induced vibration problems, such as vortex-induced vibrations in hydrofoil and runner blades (Dorfler *et al.* 2012; Liaghat *et al.* 2014). Methods for modeling fluid-structure interaction have been widely investigated (see Dowell *et al.* 2001 for a comprehensive review). In the case of guide vane torsional mode self-excited vibrations at small openings, the vibration frequencies are close to the torsional mode natural frequency in water, and high-amplitude fluctuations have been found in governor pressures during vibration incidents at sites Nennemann and Parkinson 2010. It can therefore be concluded that only the torsional mode is involved during self-excitation incidents. The torsional mode can be represented by a 1DOF oscillator, which has been modeled and validated in detail for an oscillating hydrofoil by Münch *et al.* (2008) and Münch *et al.* (2010). A similar approach, coupling the unsteady CFD method with a 1DOF oscillator, was used by Nennemann and Parkinson (2010) and Nennemann *et al.* (2012) to study guide vane vibration incidents. Torsional mode self-excited vibrations were predicted at small openings with a response frequency close to the natural torsional mode frequency in water, as observed at site tests (Nennemann and Parkinson 2010).

According to the results of previous studies, unexpected guide vane vibrations and strong noises in the small opening range with pump flow are generally related to unstable torsional mode self-excited vibrations. However, the process and mechanism of unstable self-excited vibrations have not been fully studied in previous research. Furthermore, in recent starting up tests for a high-head pump-turbine, the amplitude of guide vane vibrations and the pressure fluctuations in the radial gap decreased significantly after the starting up process was changed to one with a lower-pressure level in the radial gap area at small openings. This shows that the amplitude of guide vane torsional mode vibration is closely related to the pressure level in the radial gap. In other words, the operating conditions of the guide vane, such as the opening angle and the pressure difference between the runner side and the stay vane side, may have large effects on the instability of torsional mode self-excited vibrations. Yet the influences of guide vane operating conditions are still not clear and have not been the focus of previous studies. Therefore, in this study, numerical simulations based on the coupling of the CFD method and a 1DOF oscillator were carried out for guide vane torsional mode self-excited vibrations in a high-head prototype pump-

turbine. First, the influences of the guide vane operating conditions were analyzed and verified based on test site measurements of guide vane horizontal vibrations and pressure fluctuations in the radial gap area. Then, an energy-based analysis was conducted for torsional mode self-excited vibrations under different operating conditions. In addition, the dynamic characteristics of guide vane self-excited vibrations were examined to obtain a better understanding of how unstable torsional mode self-excited vibration occurred with pump flow at small opening angles. The results of this study will be helpful in ensuring the safety of the pump-mode starting up process and preventing mechanical damage to high-head prototype reversible pump-turbines.

## 2. NUMERICAL METHODS

### 2.1 Governing Equations

As shown in previous studies, the only vibration mode involved can be concluded to be the torsional mode. The guide vane torsional vibration only involves the angular displacement, which is caused by the elastic deformation of guide vane stem. This suggests that the spanwise flow of guide vane blade, which may be caused by end wall clearance or the flow separation at trailing edge, can be identified as axial disturbance and not considered in this study. Thus, the two-dimensional (2D) approach was considered to be a valid approximation for use in simulating the torsional mode self-excited vibration. As shown in Fig. 1, the torsional mode can be represented by a 1DOF oscillator (Münch *et al.* 2008; Münch *et al.* 2010). The torsional vibration can be processed as the rotation of the rigid body profile around the guide vane rotation axis, which avoids the structural mechanics calculation of the guide vane. The differential equation for this model is as follows

$$\ddot{\theta} + \omega_1^2 \theta = \frac{M}{J} \quad (1)$$

where  $\theta$  is the rotation degree,  $\ddot{\theta}$  is the angular acceleration,  $M$  is the hydraulic torque,  $J$  is the mass moment of inertia, and  $\omega_1$  is the natural circular frequency, calculated as follows:

$$\omega_1 = \frac{K}{J} \quad (2)$$

where  $K$  is the torsional stiffness and  $U_{ref}$  is the upstream flow velocity. In this model, the damping, which is proportional to the vibration velocity, was not considered, and neither was other external damping, such as that from mechanical friction, because these would always be positive and stabilize the self-excited vibration. Hydrodynamic damping is included in the hydraulic torque  $M$ .

The ANSYS CFX rigid body solver was employed for URANS-1DOF coupling simulations. A mass-spring system was modeled with an elastic spring model (Izhar *et al.* 2017). The first-order backward Euler algorithm was used for the rotational motion solution. Through the displacement of the guide vane

profile and the fluid moment obtained from the flow solution, the new angular position can be recalculated using the mesh deformation algorithm and influences the flow solution of the next time step. A detailed description of the rigid body solver can be found in ANSYS (2017).

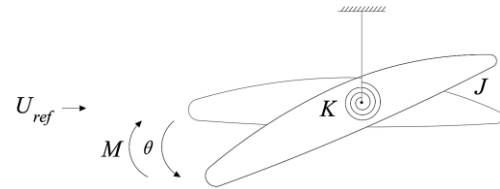


Fig. 1. Sketch of the flow-induced torsional mode vibration based on a 1DOF oscillator.

The unsteady Reynolds-averaged Navier-Stokes (URANS) solver in ANSYS CFX was used for the turbulent flow calculation. The mass conservation equation and momentum equation are shown as Eqs. (3) and (4), respectively, in both of which, all of the averaged bars are taken off except for the Reynolds stresses (Guo *et al.* 2018):

$$\frac{\partial \rho}{\partial t} + \frac{\partial}{\partial x_j} (\rho u_j) = 0 \quad (3)$$

$$\begin{aligned} & \frac{\partial}{\partial t} (\rho u_i) + \frac{\partial}{\partial x_j} (\rho u_i u_j) \\ & = -\frac{\partial p}{\partial x_i} + \frac{\partial}{\partial x_j} \left( \mu \frac{\partial u_i}{\partial t} - \overline{\rho u_i' u_j'} \right) + S_M \end{aligned} \quad (4)$$

where  $u_i$  ( $i=u, v, w$ ) is the velocity,  $x_i$  ( $i=x, y, z$ ) is the position,  $t$  is the time,  $p$  is the pressure,  $\mu$  is the dynamic viscosity, and  $S_M$  is the external momentum source term. The turbulence model of  $k-\omega$  shear stress transport (Menter 1994) was utilized in this study to model the Reynolds stresses  $\overline{\rho u_i' u_j'}$ . In this turbulence model, the Wilcox  $k-\omega$  model (Wilcox 1988) is used to calculate near-wall flow and the  $k-\epsilon$  model (Launder and Sharma 1974) is applied for main flow area. This exploits the advantages of these two turbulence mode and has a good behave on the prediction of the onset and amount of flow separation.

### 2.2 Studied Object and Numerical Settings

A reversible pump-turbine typically consists of a draft tube, a runner, adjustable guide vanes, stay vanes, and a spiral casing, as shown in Fig. 2. Small guide vane opening situations are experienced during the pump-mode starting up process, as shown in Fig. 3.

Comparative studies were carried out for two different computational domains: partial flow passage containing one guide vane (shown in Fig. 4 with red lines) and whole flow passage involving all guide vanes. The results showed that the influence of neighboring guide vanes on the self-excited vibration could be neglected in this study. Thus, the computational domain was chosen as shown in Fig. 4 for the relatively fine mesh resolution and high

simulation accuracy. The inlet was between the guide vanes and the runner, while the downstream of the computational domain was extended outward to provide better boundary conditions. The interface between two neighboring guide vanes was set with rotational periodicities.

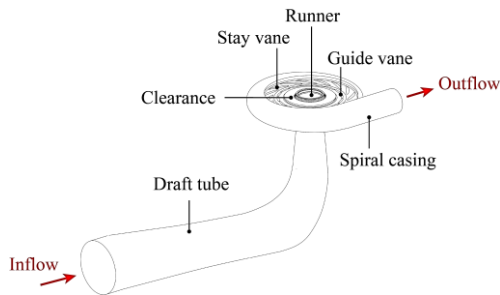


**Fig. 2. Main flow passage components of a reversible pump-turbine (pump mode).**

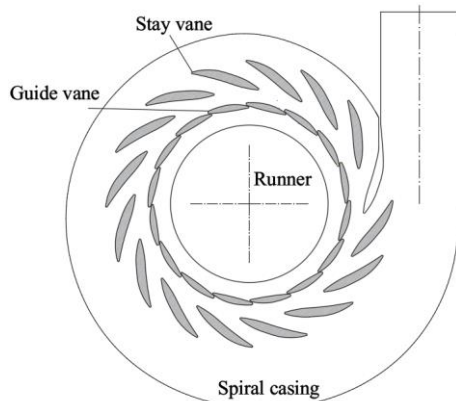


**Fig. 3. Horizontal central cross-section of the flow passage (runner removed).**

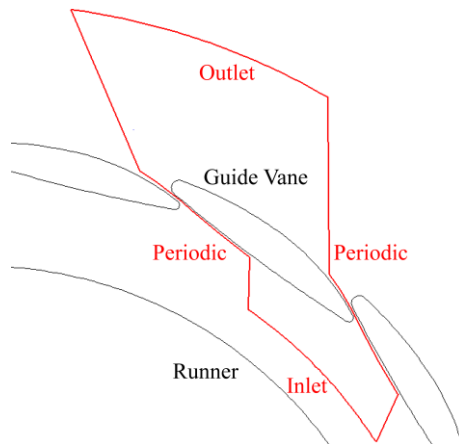


**Fig. 4. Computational domain of the guide vane torsional mode self-excited vibration**

As indicated by guide vane self-excited incidents in site tests, the self-excited vibration duration was very short, which left little time for the change of the average flow rate. Thus, the head was almost stable during the self-excited vibration process, according to the characteristic curve. This was also demonstrated by the constant average pressure measured in the radial gap area between the runner and the guide vanes. Because of the low frequency

of the flow stall in stay vanes, the outlet pressure could be considered constant during the self-excited vibration process. Based on this, the opening static pressure was set as the outlet boundary condition, which was roughly equal to the static pressure at the outlet of the spiral casing because of the very low flow rate. The total pressure set as the inlet boundary condition was calculated via steady-state RANS simulation.

The basic numerical settings are listed in Table 1. Water was set as the working fluid in the coupling calculations of the unsteady Reynolds-averaged Navier-Stokes solver with a single-degree-of-freedom oscillator model (URANS-1DOF). The automatic near-wall treatment in ANSYS CFX was employed for the guide vane wall, which automatically switched from wall function to a Low-Reynolds near-wall formulation as the mesh was refined. The guide vane profile was calculated by the rigid body solution. The 1DOF oscillator was established by setting the mass moment of inertia, the torsional stiffness, and the rotational degree of freedom. Considering the natural frequency imposed in the torsional spring model, a time step of  $\Delta t = 1.875 \times 10^{-4}$  s was used to ensure adequate resolution to the response frequency. A detailed description of the numerical methodology can be found in ANSYS (2017).

**Table 1 Basic numerical settings of URANS-1DOF coupling simulations**

Item	Setting
Inlet boundary condition	Total pressure
Outlet boundary condition	Static pressure
Mesh motion of guide vane	Rigid body solution
External torque	1DOF torsional spring
Wall function	Automatic near-wall treatment
Advection scheme	High resolution
Turbulence numeric	High resolution
Transient scheme	Second-Order Backward Euler
Convergence criterion	Root-mean-square residual below $1 \times 10^{-5}$
Maximum number of the inner loop	20

### 2.3 Mesh Generation and Independence

In the present work, hexahedral structured meshes were generated using ICEM-CFD to discretize the computation domain. Three meshing cases were used to evaluate the mesh resolution using the grid convergence index (GCI) method based on the Richardson extrapolation. A detailed description of the GCI method can be found in Celik *et al.* (2008). As shown in Section 3.2, the torsional mode self-excited vibration under operating conditions of  $\alpha_0=0.2^\circ$  and  $\delta\psi=1.116$ , where  $\alpha_0$  is the initial guide vane opening angle and  $\delta\psi$  is the pressure difference between the inlet (runner side) and outlet (stay vane

side), was more unstable than under the other conditions considered. Thus, a mesh resolution sufficient for the operating conditions of  $\alpha_0=0.2^\circ$  and  $\delta\psi=1.116$  was assumed to be applicable to the other operating cases as well. URANS-1DOF coupling calculations were carried out based on the steady-state RANS results. To evaluate the instability of self-excited vibration, a damping ratio was defined as follows:

$$\zeta_\alpha = \frac{\ln(\alpha_P / \alpha_R)}{2\pi N} \quad (5)$$

where  $\alpha$  is the guide vane opening angle, the subscript P and R represent two peaks with an interval of  $NT$  ( $N=1, 2, \dots$ ), and  $T$  is the vibrating period, as shown in Fig. 5. A negative value of the damping ratio means the self-excited vibration is unstable. The velocity  $C_{v\_thr}$  at the narrow gap throat between two guide vanes was chosen as the key variable ( $\chi$ ) for the steady-state RANS simulation results, and the damping ratio  $\zeta_\alpha$  as chosen for the URANS-1DOF coupling calculation results. The calculations of the discretization error for the mesh are shown in Table 2. The convergence index of  $GCI_{fine}^{21}$  was within 5%. Thus, a mesh number of  $N_I=81,201$  was considered acceptable in this study. In the partial computational cells shown in Fig. 6, the meshes were intentionally refined in the narrow gap and near the trailing edge (pump mode). The value of  $y_{plus}$ , a classical non-dimensional distance for wall-bounded flow, was less than 30 for the guide vane wall.

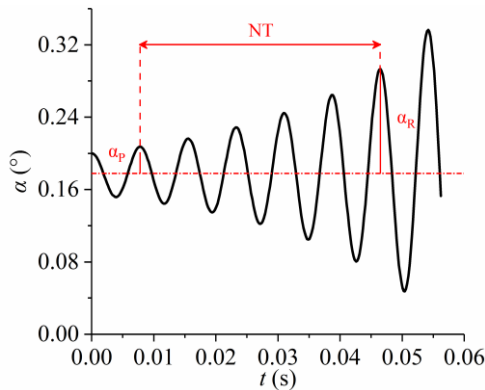


Fig. 5. Definition of the damping ratio of torsional mode self-excited vibration.

Table 2 Calculations of the discretization error for the meshes

Item	$C_{v\_thr}$	$\zeta_\alpha$
$N_1, N_2, N_3$	81201, 47025, 26532	
$r_{21}$	1.314	
$r_{32}$	1.331	
$\chi_1$	1.794	-0.04464
$\chi_2$	1.824	-0.05635
$\chi_3$	1.844	-0.05798
$\phi_{ext}^{21}$	1.739	-0.0430
$e_{ext}^{21}$	3.17%	3.86%
$GCI_{fine}^{21}$	3.85%	4.65%

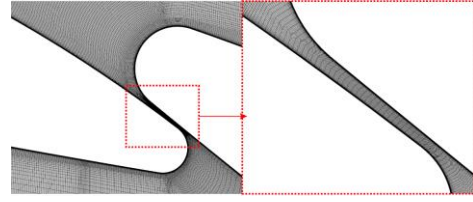


Fig. 6. Partial computational cells of the guide vane torsional mode self-excited vibration.

### 3. RESULTS AND DISCUSSION

#### 3.1 Overview of the Guide Vane Torsional Mode Vibrations in Site Tests

For a prototype reversible pump-turbine, the rotating speed of the runner begins to increase from 0 to 100% (with approximately 20% power load) during the pump-mode starting up process. During this period, the pressure in the runner chamber is maintained with pressurized air to avoid instant overload. When the rotating speed reaches 100%, the ball valve starts opening while the air is released out of the runner chamber. Finally, the load increases to the full load when the ball valve and the guide vane are completely opened.

As shown in Fig. 7, two different starting up cases were examined in recent pump-mode site tests to reflect two different processes for opening the guide vane after the ball valve started to open. In starting up process A, the guide vane stayed closed for approximately 45.5 s and thereafter opened steadily from 0 to 100%. In starting up process B, the guide vane first pre-opened from 0 to approximately 4.8%, maintained that degree of opening for approximately 15.5 s, and then opened steadily to 100%. The pressure pulsations measured at the radial gap (between the runner and the guide vanes) are shown in Fig. 8 for guide vane openings from 0 to approximately 4.8%. The amplitude of the pressure pulsation was larger for starting up process A than for process B, especially for the small opening ranges, and then decreased as the guide vane continued to open.

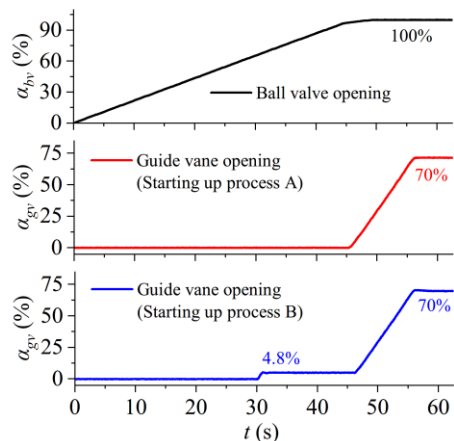
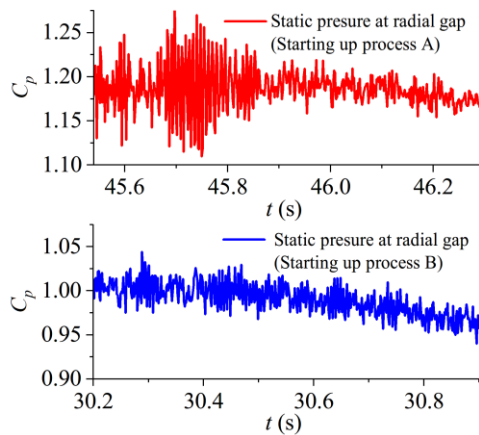
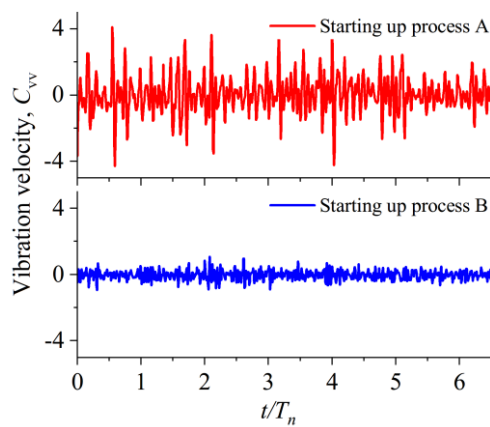


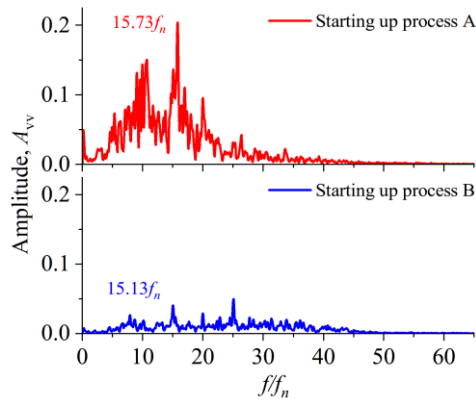
Fig. 7. Time histories of the guide vane openings after the ball valve starts to open.



**Fig. 8. Time histories of the pressure pulsations at the radial gap while the guide vane is opening from 0 to around 4.8%.**



a) Time histories of the vibration velocities, where  $T_n$  is the runner rotating period



b) Amplitudes of the vibration velocities, where  $f_n$  is the runner rotating frequency

**Fig. 9. Horizontal vibration velocities of the guide vane blade in site tests while the guide vane is opening from 0 to around 4.8%.**

The horizontal vibration velocities of the guide vane blades were also found to have large amplitudes during starting up process A. In this study, the guide vane with the largest vibration amplitude was chosen for use in evaluating the guide vanes' vibrations in the pump-turbine. Figure 9 shows the time histories and amplitudes of the vibration velocity of this guide

vane, where  $C_{vv}$  and  $A_{vv}$  are the vibration velocity values that were nondimensionalized by the peak-to-peak value of the vibration velocity in starting up process B.

Analysis shows that the main frequencies of the pressure pulsation and the vibration velocity during starting up process A are both approximately equal to the torsional mode natural frequency of the guide vane in water ( $15.73f_n$ ). The high-amplitude vibration of the guide vane during the small opening range of starting up process A is considered to be the torsional mode self-excited vibration (hereinafter referred to as the self-excited vibration). In addition, the average pressure at the radial gap in the small opening ranges of starting up process A was much higher than that of starting up process B. Thus, it can be concluded that torsional mode self-excited vibration is much more likely to be unstable when the guide vane opening is small and the average pressure at the runner outlet is high. In other words, the operating conditions of the guide vane, including the opening angle and the pressure difference between the runner side and the stay vane side, are closely related to the instability of the self-excited vibration.

The detailed observations on the vibration and flow field are difficult to conduct at this point, because the torsional vibration usually occurs in a high-head prototype pump-turbine. Thus the above conclusive experimental evidences on pressure pulsations and guide vane vibration were used for the qualitative validation of URANS-1DOF coupling simulations.

### 3.2 Influences of the Operating Conditions on Guide Vane Self-Excited Vibrations

Coupling simulations of URANS-1DOF were carried out at different guide vane initial opening angles ( $\alpha_0$ ) and inlet-outlet pressure difference ( $\delta\psi$ ), as shown in Table 3. Case 1 was chosen as the center group of the orthogonal studies, in which the pressure difference  $\delta\psi = 1.116$  was calculated by steady-state RANS for the flow rate of  $\alpha_0 = 0.2^\circ$ .

**Table 3 Operating conditions**

Case	$\alpha_0$ ( $^\circ$ )	$\delta\psi$
1	0.2 $^\circ$	1.116
2	0.4 $^\circ$	1.116
3	0.6 $^\circ$	1.116
4	1 $^\circ$	1.116
5	0.2 $^\circ$	0.925
6	0.2 $^\circ$	0.728
7	0.2 $^\circ$	0.422
8	0.2 $^\circ$	0.189

Based on the steady-state RANS results, the contours of the static pressure and the velocity near the narrow gap in case 1 are shown in Fig. 10. Because of the slight opening and the high pressure difference, the narrow gap flow is attached to the next guide vane surface and leads to large gradients of static pressure and velocity.

The static pressure ( $C_{p\_thr}$ ) and velocity magnitude ( $C_{v\_thr}$ ) at the throat of the narrow gap and the total hydraulic torque on the guide vane ( $C_\tau$ ) were plotted

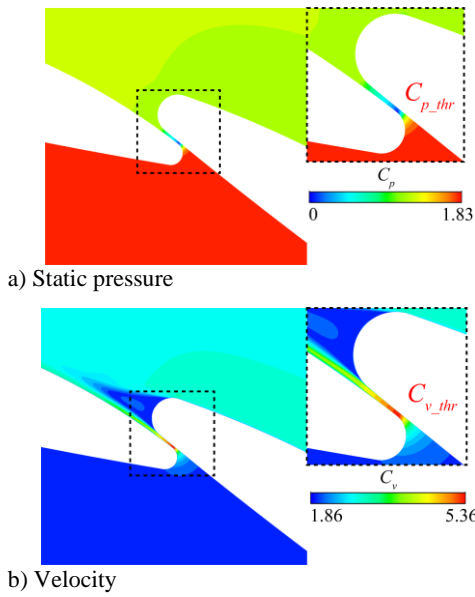


**Fig. 10. Contours of the static pressure and velocity near the narrow gap under  $\alpha_0=0.2^\circ$  and  $\delta\psi=1.116$ .**

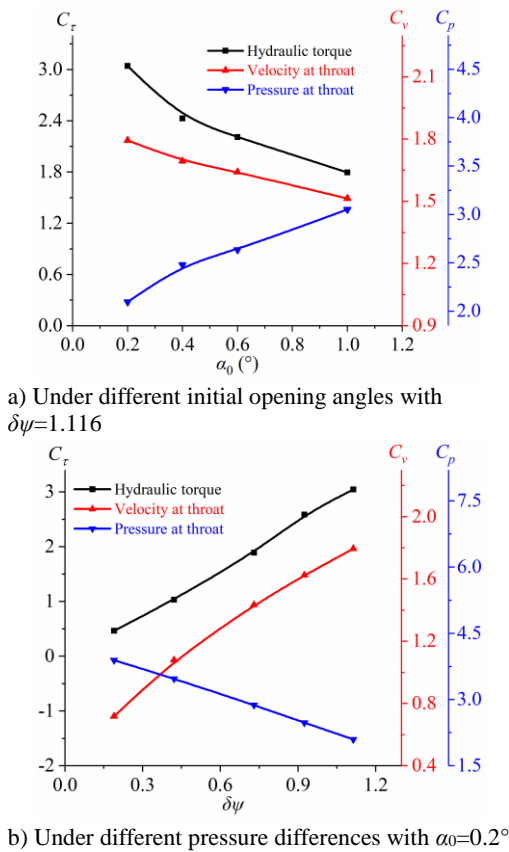


**Fig. 11. Static pressures and velocity magnitudes at the throat and total hydraulic torques under different operating conditions.**

for different conditions, as shown in Fig. 11. The high-speed flow in the narrow gap is strengthened as the opening angle decreased or pressure difference increased. Because of the larger pressure drop in the narrow gap, the total hydraulic torque on the guide vane (a positive value corresponds to the closing

direction of the guide vane) is larger under conditions of smaller opening angles or higher pressure differences.

Figure 12 presents the damping ratios  $\zeta_\alpha$  for different opening angles and pressure differences. The time histories of the stable and unstable self-excited vibrations are also shown for some typical operating conditions. The vibration frequencies are in the ranges of  $15.6 f_n$  to  $16.1 f_n$ , which is consistent with the main frequency of the guide vane horizontal vibration velocity in the site test for starting up process A. The damping ratio declines as the initial opening angle decreases or the pressure difference increases. The values of  $\zeta_\alpha$  are negative when  $\alpha_0 \leq 0.6^\circ$  or  $\delta\psi \geq 0.422$  and positive under other operating conditions. This suggests that guide vane self-excited vibrations are unstable and that it is possible to develop high-amplitude vibrations at small initial opening angles and high pressure differences. As the opening angle increases or the pressure difference decreases, the self-excitation instability is gradually weakened and considered to be stable in cases 4 and 8.

These results agree well with the conclusive experimental evidences of the site test with starting up process A. Therefore, the coupling simulations were considered to be acceptable for analyzing the influences of guide vane operating conditions, at least qualitatively.

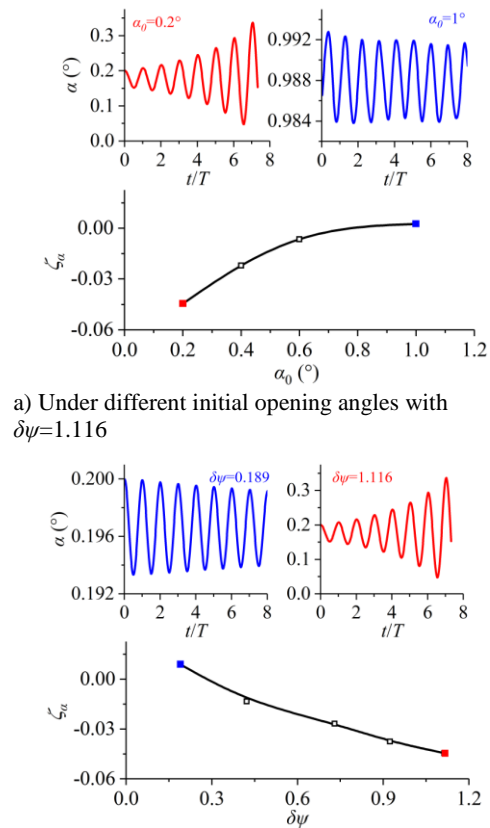


**Fig. 12. Damping ratios and time histories of the self-excited vibrations under different operating conditions, where  $T$  is the period of self-excited vibration.**

### 3.3 Energy-Based Analysis on Guide Vane Self-Excited Vibrations

The fluid force on the guide vane was evaluated using the total hydraulic torque  $M$ . The work done by the hydraulic torque during one time step (from  $t_{m-1}$  to  $t_m$ ) is calculated as follows:

$$W_m = \frac{(\tau_{m-1} + \tau_m)\theta_m}{2} = -\frac{(\tau_{m-1} + \tau_m)(\alpha_m - \alpha_{m-1})}{2} \quad (6)$$

where  $m$  ( $m=1, 2, \dots$ ) is the current time step,  $t_m = m \times \Delta t$  is the current time,  $\tau_m$  is the current total hydraulic torque,  $\theta_m$  is the degree of rotation during one time step, and  $\alpha_m$  is the current opening angle. A positive value of  $W_m$  means that the direction of total hydraulic torque is the same as that of guide vane rotation. Taking the case of  $\alpha_0=0.2^\circ$  and  $\delta\psi=1.116$  as an example, the time history of the work done by the total hydraulic torque is shown in Fig.13. The different stages are marked as Stages I and II. The work fluctuates at a single frequency in Stage I but contains a higher-frequency component in Stage II, in addition to the basic frequency. This is caused by the negative minimum value of total hydraulic torque when the fluctuating amplitude is large, as shown in Fig. 14.

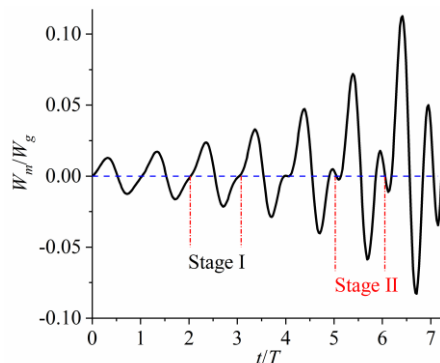


Fig. 13. Time history of the work done by total hydraulic torque under the condition of  $\alpha_0=0.2^\circ$  and  $\delta\psi=1.116$ .

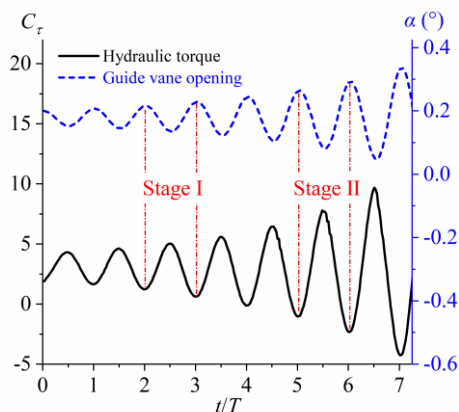


Fig. 14. Time histories of the total hydraulic torque and guide vane opening angle under the condition of  $\alpha_0=0.2^\circ$  and  $\delta\psi=1.116$ .

During the self-excited vibration process, the remaining energy after one vibrating period exists in the form of guide vane rotating kinetic energy and the elastic energy stored in the torsional spring. To evaluate the cumulative effect of the work done by the total hydraulic torque, a new variable is defined as follows:

$$\sum W = \sum_{m=0}^n W_m \quad (7)$$

where  $n$  ( $n=1, 2, \dots$ ) is the cumulative number of time steps. The cumulative work  $\sum W$  represents the sum of the work done by the total hydraulic torque during the cumulative period from 0 to  $t_n=n\Delta t$ . A positive value of  $\sum W$  indicates that the positive work done by the total hydraulic torque is larger than the negative work.  $\sum W$  was calculated when the vibration period was an integer, that is,  $t_n=NT$  ( $N=1, 2, \dots$ ). Considering the effect of the elasticity of the 1DOF torsional spring, the cumulative work  $\sum A$ , representing the sum of the work done by the elastic torque, could be calculated using a similar approach.

Time histories of the cumulative work  $\sum W$  and  $\sum A$  are shown in Fig. 15 for different operating conditions.  $\sum W$  decreases slowly with time under operating conditions corresponding to positive damping ratios ( $\alpha_0=1^\circ$  in Fig. 15(a) and  $\delta\psi=0.189$  in Fig. 15(b)) and increases gradually under operating conditions corresponding to negative damping ratios.  $\sum A$  is negative under all operating conditions, indicating that the elastic torque plays a role in damping during the self-excitation process. Under the condition of a negative damping ratio, the large torsional displacement of the guide vane results in a large impedance effect of the elastic torque. What is striking in the figures is the dramatically increasing trend of the cumulative work  $\sum W$  when  $\alpha_0=0.2^\circ$  and  $\delta\psi=1.116$ . These results suggest that the total hydraulic torque plays a role in inputting energy into guide vane rotation and then intensifying the self-excited vibration.

The stability of guide vane self-excited vibration depends on both the total hydraulic torque and the torsional spring elastic torque. Because of the larger positive values of  $\sum W$  than of  $\sum A$ , the self-excited vibrations are unstable under the operating conditions corresponding to negative damping ratios. For the operating conditions corresponding to positive damping ratios, the self-excited vibrations become stable because of the stronger impeding effect of the elastic torque than the driving effect of the total hydraulic torque.

### 3.4 Dynamic characteristics of guide vane self-excited vibrations

Phase differences between the total hydraulic torque and the guide vane angular velocity under different operating conditions are shown in Fig. 16. The phase differences are less than  $90^\circ$  when  $\alpha_0 \leq 0.6^\circ$  or  $\delta\psi \geq 0.422$ . For the operating conditions of  $\alpha_0=1^\circ$  in Fig. 16(a) and  $\delta\psi=0.189$  in Fig. 16(b), the phase differences are greater than  $90^\circ$ .

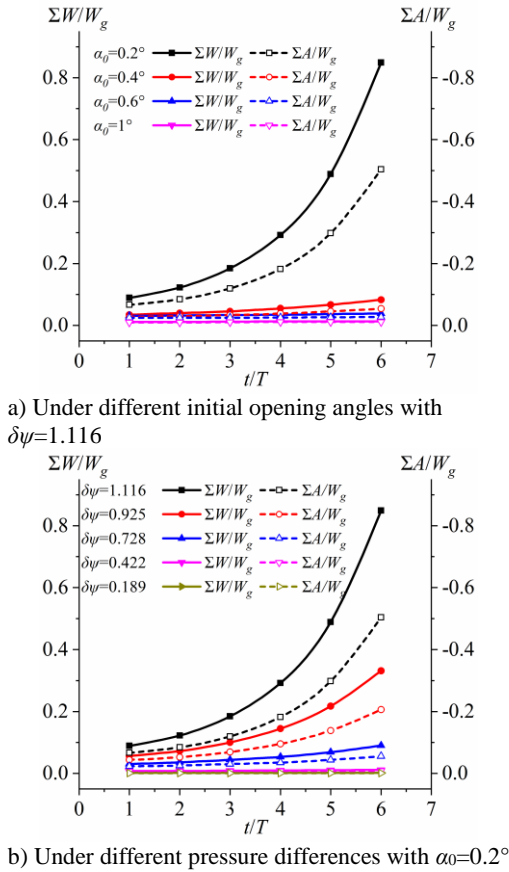


**Fig. 15. Time histories of the accumulated work  $\Sigma W$  and  $\Sigma A$  under different operating conditions.**

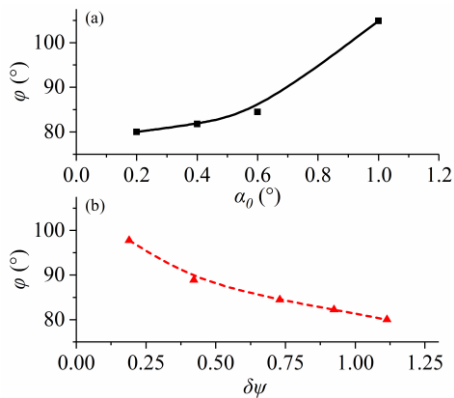


**Fig. 16. Phase differences between total hydraulic torque and guide vane angular velocity: (a) under different initial opening angles with  $\delta\psi=1.116$ ; (b) under different pressure differences with  $\alpha_0=0.2^\circ$ .**

To analyze how the phase difference affects the stability of guide vane self-excited vibration, the work done by the total hydraulic torque on guide vane rotation around its axis during one vibration period  $T$  can be expressed as follows:

$$W_T = \int_0^T \tau(t) \cdot \omega(t) dt \quad (8)$$

where  $\tau$  is the fluctuating total hydraulic torque and  $\omega$  is the fluctuating angular velocity. Assuming that

the total hydraulic torque and the guide vane angular velocity vary according to sinusoidal waveforms during one self-excited vibration period, Eq. (8) can be expressed as follows:

$$\begin{aligned} W_T &= \int_0^T A_\tau \sin\left(\frac{2\pi}{T}t - \varphi\right) \cdot A_\omega \sin\left(\frac{2\pi}{T}t\right) dt \\ &= 0.5A_\tau A_\omega T \cos \varphi \end{aligned} \quad (9)$$

where  $A_\tau$  and  $A_\omega$  are the fluctuating amplitudes of the total hydraulic torque and the guide vane angular velocity, respectively, and  $\varphi$  is the phase difference between the total hydraulic torque and the angular velocity.  $W_T$  is positive if the phase difference  $\varphi$  is less than  $90^\circ$ , such as in the cases of  $\alpha_0 \leq 0.6^\circ$  or  $\delta\psi \geq 0.422$ . This leads to energy accumulation during one vibration period. In contrast, if the phase difference is greater than  $90^\circ$ , the total hydraulic torque has a damping effect on the guide vane vibration, such as in the cases of  $\alpha_0=1^\circ$  and  $\delta\psi=0.189$  in Fig.16(b), as shown in Figs. 16(a) and 16(b), respectively.

The relation between the guide vane opening angle and the total hydraulic torque is also helpful in understanding the unstable self-excited vibration. Taking the condition of  $\alpha_0=0.2^\circ$  and  $\delta\psi=1.116$  as an example, the curves of total hydraulic torque as a function of guide vane opening angle are different for the closing process and the opening process in both Stages I and II, as shown in Fig. 17. Points (a, C) encircle in a counter-clockwise direction with time. The value difference between the closing process and the opening process is positively correlated to the energy accumulation in one vibration period. This value difference is larger in Stage II than in Stage I. This implies that the energy accumulation is also related to the guide vane vibration amplitude or the angular velocity. A qualitative explanation can be understood from Eq. (9), in which the work done by the total hydraulic torque in one vibration period is also related to the fluctuating amplitudes of the total hydraulic torque ( $A_\tau$ ) and the guide vane angular velocity ( $A_\omega$ ). For the higher-amplitude vibration period, the larger values of  $A_\tau$  and  $A_\omega$  result in larger values of  $W_T$ . This in turn leads to an increase in the vibration amplitude of the next period. Thus, it is concluded that there is positive feedback between the guide vane vibration amplitude and the energy accumulation in one vibration period.

Under the operating conditions of small initial opening angles and high pressure differences, the phase differences between the total hydraulic torque and the guide vane angular velocity are smaller than  $90^\circ$ , which leads to the energy accumulation in each vibration period. Because of the positive feedback between vibration amplitude and energy accumulation, an increasing vibration amplitude contributes to energy accumulation and then leads to a higher amplitude during the next vibration period. Thus, unstable self-excited vibrations are induced under these operating conditions, considering the smaller damping effect of the torsional spring. For the cases of large initial openings or low pressure differences, the negative work done by the total hydraulic torque dampens the guide vane vibration

and gradually stabilizes the self-excited vibration. These findings are in good agreement with the qualitative conclusions drawn from the results of the starting up tests described in Section 3.1, in which the strong pressure fluctuations and the horizontal vibration velocity of the guide vane blade are more likely to occur under the operating conditions of small guide vane openings and high pressures in the radial gap area between the guide vane and the runner. For this reason, a starting up process with a high pressure level at the runner outlet should be avoided for high-head prototype pump-turbines. In other words, reducing the pressure level at the runner outlet by changing the starting up operating process (such as pre-opening guide vanes) is an effective way of preventing the high-amplitude guide vane vibrations and the strong pressure fluctuations in the small opening range during the pump mode's starting up process.

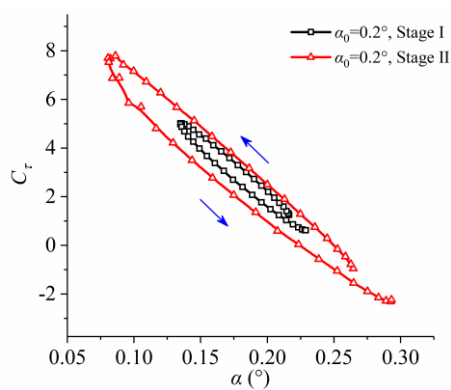


**Fig. 17. Total hydraulic torques vs. guide vane opening angles in Stage I and Stage II under  $\alpha_0=0.2^\circ$  and  $\delta\psi=1.116$ .**

#### 4. CONCLUSIONS

The current study aimed to investigate the relationship between the operating conditions and guide vane self-excited vibration in a reversible pump-turbine when running at small openings during the pump-mode starting up process. Coupling simulations, based on the unsteady CFD method with a 1DOF oscillator, were carried out for the guide vane of a high-head prototype reversible pump-turbine under different operating conditions. The following conclusions can be drawn:

- (1) Operating conditions, including the initial opening angle and the pressure difference between the runner side and the stay vane side, significantly affect the instability of guide vane self-excited vibrations. The self-excited vibrations are unstable and can develop into high-amplitude vibrations under conditions of relatively small opening angles and high pressure differences. Combined with the qualitative conclusions of starting up site tests, the results show that reducing the pressure level in the radial gap between guide vanes and the runner is effective in avoiding high-amplitude guide

vane vibration and strong pressure fluctuations in the small opening range.

- (2) Energy-based analyses were conducted for stable and unstable self-excited vibrations. The positive work done by the total hydraulic torque is larger than the impeding effect of the torsional spring elasticity for cases of negative damping ratios. This results in energy accumulation and is responsible for unstable self-excited vibrations.
- (3) Further analysis of the dynamic characteristics of guide vane self-excited vibrations shows that the phase differences between the total hydraulic torque and the guide vane angular velocity are less than  $90^\circ$  for small openings and high pressure differences. This is considered to be one of the root causes of the energy accumulation in one vibration period. In addition, there is positive feedback between guide vane vibration amplitude and energy accumulation, which would aggravate the development of unstable self-excited vibration.

The coupling simulations conducted in this study did not take into account the transient influences of the pump-mode starting up process, which may affect the characteristics of guide vane self-excited vibration. Further investigation of this point is needed in the future.

#### ACKNOWLEDGEMENTS

This work was supported by the National Natural Science Foundation of China (Grant no. 52079141).

#### REFERENCES

- ANSYS (2017). *ANSYS CFX-Solver Modeling Guide: Release 18.0*. ANSYS Inc., Canonsburg, United States.
- Celik, I. B., U. Ghia, P. J. Roache and C. J. Freitas (2008). Procedure for estimation and reporting of uncertainty due to discretization in CFD applications. *Journal of Fluids Engineering* 130, 078001.
- Dörfler, P., M. Sick and A. Coutu (2013). *Flow-induced pulsation and vibration in hydroelectric machinery: engineer's guidebook for planning, design and troubleshooting*. Springer, London, UK.
- Dowell, E. H. and K. C. Hall (2001). Modeling of fluid-structure interaction. *Annual Review of Fluid Mechanics* 33(1), 445-490.
- Guo, Q., L. Zhou, Z. Wang, M. Liu and H. Cheng (2018). Numerical simulation for the tip leakage vortex cavitation. *Ocean Engineering* 151, 71-81.
- Izhar A., A. H. Qureshi and S. Khushnood (2017). Simulation of vortex-induced vibrations of a

- cylinder using ANSYS CFX rigid body solver. *China Ocean Engineering* 31(1), 79-90.
- Lauder, B. E. and B. I. Sharma (1974). Application of the energy-dissipation model of turbulence to the calculation of flow near a spinning disc. *Letters in Heat and Mass Transfer* 1(2), 131-137.
- Li, Z., H. Bi, B. Karney, Z. Wang and Z. Yao (2017). Three-dimensional transient simulation of a prototype pump-turbine during normal turbine shutdown. *Journal of Hydraulic Research* 55(4), 520-537.
- Liaghat, T., F. Guibault, L. Allenbach and B. Nennemann (2014, November). Two-way fluid-structure coupling in vibration and damping analysis of an oscillating hydrofoil. *Proceedings of ASME International Mechanical Engineering Congress and Exposition*, Quebec, Canada, V04AT04A073.
- Menter, F. R. (1994). Two-equation eddy-viscosity turbulence models for engineering applications. *AIAA Journal* 32(8), 1598-1605.
- Münch, C., P. Ausoni, O. Braun, M. Farhat and F. Avellan (2008, October). Hydro elastic behavior of vibrating blades. *Proceedings of the 24th symposium on hydraulic machinery and systems*, Iguassu, Argentina.
- Münch, C., P. Ausoni, O. Braun, M. Farhat and F. Avellan (2010). Fluid-structure coupling for an oscillating hydrofoil. *Journal of Fluids and Structures* 26(6), 1018-1033.
- Nennemann B. and E. Parkinson (2010). YiXing pump-turbine guide vane vibrations: problem resolution with advanced CFD analysis. *IOP Conference Series: Earth and Environmental Science* 12(1), 012057. IOP Publishing, London, UK.
- Nennemann, B., M. Sallaberger, U. Henggeler, C. Gentner and E. Parkinson (2012). Assessment of guide vane self-excitation stability at small openings in pump flow. *IOP Conference Series: Earth and Environmental Science* 15(6), 062032. IOP Publishing, London, UK.
- Oishi, A. and T. Yokoyama (1980, January). Development of high-head single-and double-stage reversible pump-turbines. *Proceedings of 10th IAHR Symposium on Hydraulic Machinery and Cavitation*, Tokyo, Japan, 441-452.
- Pulpitel, L. (1982, September). Self-excited vibration of pump-turbine guide vanes. *IAHR 11th Symposium on Hydraulic Machinery, Equipment and Cavitation*, Amsterdam, Netherlands.
- Rau, N. S. (1994). *The State of Energy Storage in Electric Utility Systems and Its Effect on Renewable Energy Resources*. Report, National Renewable Energy Lab., Golden, United States.
- Roth, S., V. Hasmatuchi, F. Botero, M. Farhat and F. Avellan (2010, August). Advanced instrumentation for measuring fluid-structure coupling phenomena in the guide vanes cascade of a pump-turbine scale model. *Proceedings of the ASME 2010 3rd Joint US-European Fluids Engineering Summer Meeting and 8th International Conference on Nanochannels, Microchannels, and Minichannels*, Montreal, Canada, 585-597.
- Roth, S., V. Hasmatuchi, F. Botero, M. Farhat and F. Avellan (2011, October). Influence of the pump-turbine guide vanes vibrations on the pressure fluctuations in the rotor-stator vaneless gap. *Proceedings of the 4th International Meeting on Cavitation and Dynamic Problems in Hydraulic Machinery and Systems*, Belgrade, Serbia, 1-11.
- Tanaka, H. and S. Tsunoda (1980, January). The development of high head single stage pump-turbines. *Proceedings of 10th IAHR Symposium on Hydraulic Machinery and Cavitation*, Tokyo, Japan, 429-440.
- Tao, R., X. Zhou, B. Xu and Z. Wang (2019). Numerical investigation of the flow regime and cavitation in the vanes of reversible pump-turbine during pump mode's starting up. *Renewable Energy* 141, 9-19.
- Wilcox, D. C. (1988). Reassessment of the scale-determining equation for advanced turbulence models. *AIAA Journal* 26(11), 1299-1310.
- Zhang, Y., Y. Zhang and T. Wu (2017). A review of rotating stall in reversible pump-turbine. *Proceedings of the Institution of Mechanical Engineers, Part C: Journal of Mechanical Engineering Science* 231(7), 1181-1204.
- Zuo, Z., S. Liu, Y. Sun and Y. Wu (2015). Pressure fluctuations in the vaneless space of High-head pump-turbines—A review. *Renewable and Sustainable Energy Reviews*, 41(2015), 965-974.